THE JOURNAL OF PHYSICAL CHEMISTRY Letters

pubs.acs.org/JPCL Letter

Time-Resolved Vibrational Fingerprints for Two Silver Cluster-DNA Fluorophores

Yuyuan Zhang, Chen He, Jeffrey T. Petty,* and Bern Kohler*

Cite This: J. Phys. Chem. Lett. 2020, 11, 8958−8963 Read Online

ACCESS | Metrics & More | Article Recommendations | Supporting Information

ABSTRACT: DNA-templated silver clusters are chromophores in which the nucleobases encode the cluster spectra and brightness. We describe the coordination environments of two nearly identical Ag_{10}^{6+} clusters that form with 18-nucleotide strands CCCCA CCCCT CCCX TTTT, with X = guanosine and inosine. For the first time, femtosecond time-resolved infrared (TRIR) spectroscopy with visible excitation and mid-infrared probing is used to correlate the response of nucleobase vibrational modes to electronic excitation of the metal cluster. A rich pattern of transient TRIR peaks in the 1400−1720 cm^{-1} range decays synchronously with the visible emission. Specific infrared signatures associated with the single guanosine/inosine along with a subset of cytidines, but not the thymidines, are observed. These fingerprints suggest that the network of bonds between a silver cluster adduct and its polydentate DNA ligands can be deciphered to rationally tune the coordination and thus spectra of molecular silver chromophores.

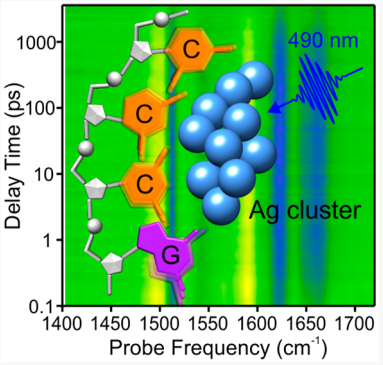

Silver clusters with ≲20 atoms are chromophores whose valence electrons organize into sparse energy levels with distinct electronic transitions and efficient fluorescence.[1−5] Although bare silver clusters are highly reactive, they can be trapped by a range of ligands, and DNA strands are particularly interesting because they not only protect but also encode the spectra of a cluster adduct.[5−9] For oligonucleotides with 10−30 nucleobases, different primary sequences tune the cluster spectra across the visible/near-infrared region, and different secondary structures modulate emission quantum yields as much as 1000-fold.[10−14] The ability to exquisitely control a cluster's spectrum and brightness has led to applications in biosensing,[15] live cell imaging,[16] and DNA photonics,[17] but a lack of knowledge about fundamental photophysical events has impeded the rational design and further development of this new class of fluorophores.

We are beginning to learn about key factors that control the electronic spectra and structure of DNA-bound silver clusters and how their emission is programmed by polydentate oligonucleotide ligands. Prior transient absorption and two-color excitation experiments have revealed several types of excited electronic states, including short-lived Franck−Condon excited states initially populated by photoexcitation, emissive excited states with nanosecond lifetimes, and even longer-lived dark excited states.[18,19] The emissive states of the clusters can relax radiatively with ≲5 ns lifetimes and with ≲90% quantum yields.[10,20,21] The dark state population persists for tens of microseconds and can be excited with a second, near-infrared laser to repopulate the emissive state, thereby enhancing fluorescence brightness.[22−26] Precisely how these states are populated from the Franck−Condon excited states and on what time scales is still uncertain, although several studies have reported ultrafast relaxation that takes place in tens of femtoseconds to tens of picoseconds.[18,27−30]

Importantly, the electronic states of a cluster are known to be strongly coupled with those of the aromatic nucleobases of its DNA host because DNA-specific UV excitation promptly yields cluster emission.[30,31] Time-dependent density functional theory (TD-DFT) calculations on molecular silver clusters cross-linked by cytosine pairs (e.g., C−Ag_n−C, n = 1−6),[32] on a Ag_4 cluster bound to an A·T or G·C base pair,[33] and on Ag_4, Ag_5^+, and Ag_6^{2+} clusters stabilized by two $(dC)_6$ strands[34] predict many transitions involving frontier orbitals with mixed silver cluster (AgC) and DNA character. Although calculations like these provide insight into base-silver cluster couplings, it is difficult to ascertain experimentally which bases are coupled most strongly.

Here, we report that ultrafast time-resolved IR (TRIR) experiments on DNA-AgCs reveal bleaching of the vibrational modes of select nucleobases when the cluster is electronically excited, yielding a mid-infrared fingerprint of the coordination site. We focused on the two strands 5′-$C_4AC_4TC_3XT_4$-3′ where X is guanosine (G) or its analog inosine (I) that lacks the exocyclic C2-NH_2 (Figure 1). Both oligonucleotides form the same Ag_{10}^{6+} adducts, as determined by negative-mode

Received: August 14, 2020
Accepted: October 1, 2020
Published: October 8, 2020

https://dx.doi.org/10.1021/acs.jpclett.0c02486
J. Phys. Chem. Lett. 2020, 11, 8958−8963

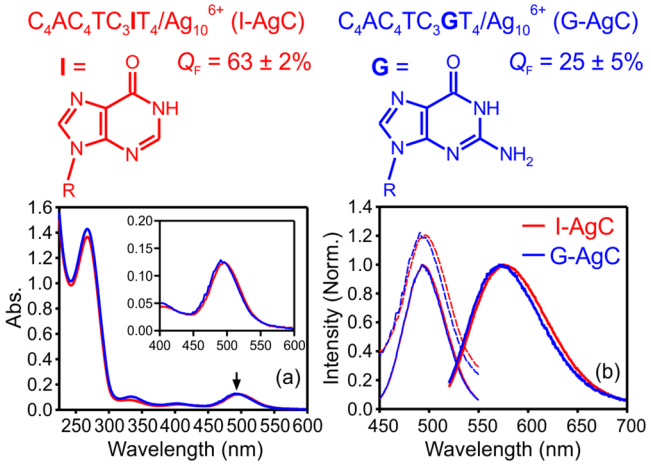

Figure 1. (a) UV−visible absorption spectra of the I-AgC (red) and G-AgC (blue) DNA-encapsulated silver clusters in 5 mM, pH = 7 cacodylate H_2O buffer solutions. Excitation wavelength (490 nm) for fs-TA and fluorescence measurements is indicated by a black arrow. Inset: The same spectra zoomed in at the 490 nm peak. (b) Normalized excitation (recorded at a fixed emission wavelength of 570 nm) and emission (following 490 nm excitation) spectra and normalized UV−visible spectra (dashed lines; offset vertically by 0.2) of I-AgC (red) and G-AgC (blue). The sequences of the DNA hosts, the chemical structures of I and G, and the fluorescence quantum yields (Q_F) of the DNA-AgC from ref 35 are shown above the spectra.

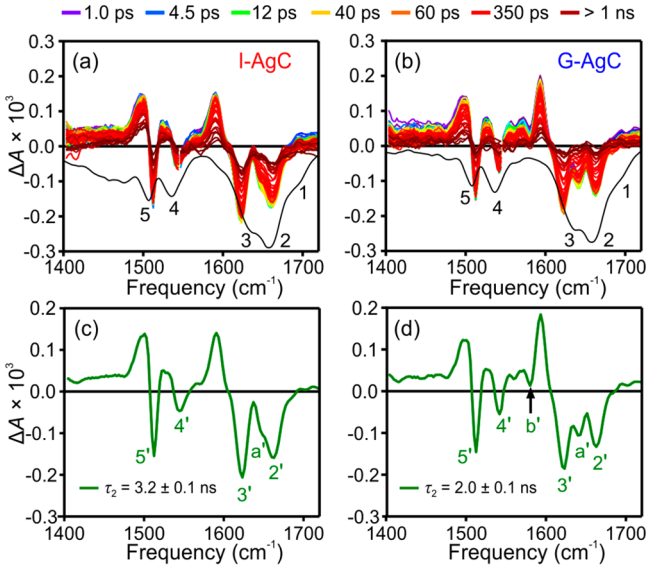

Figure 2. (a, b) Composite TRIR spectra of I-AgC and G-AgC, respectively, in 5 mM cacodylate D_2O buffer recorded at the indicated delay times following excitation by a 490 nm femtosecond pump pulse. The inverted FTIR spectra are shown for comparison. (c, d) Decay-associated difference spectra (DADS) of I-AgC and G-AgC, respectively, obtained by globally fitting the TA data from 0.5 ps to 3.5 ns. Data were fit to a biexponential decay function $\Delta A(t) = A_1 \exp(-t/\tau_1) + A_2 \exp(-t/\tau_2)$, and uncertainties are twice the estimated standard deviation (2σ). The dominant τ_2 decay components are shown here; the DADS for the τ_1 components are shown in Figure S2. Peaks labeled with numbers in the FTIR spectra (a, b) and ones labeled with letters in the TRIR spectra (c, d) are discussed in the main text.

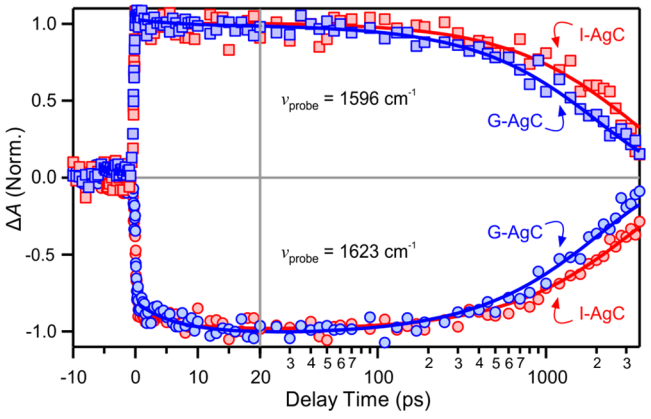

Figure 3. Normalized TRIR kinetic traces for I-AgC (red) and G-AgC (blue) with excitation at 490 nm and probing at the most intense negative band at 1623 cm^{-1} (band 3′ in Figure 2c,d) and the most intense positive band at 1596 cm^{-1}. The circles and squares are TRIR data, and the solid curves are exponential fits. The vertical line marks the linear-logarithmic axis break at 20 ps.

electrospray ionization mass spectrometry (Figure S1).[36−39] These strands also harbor similar binding sites because both Ag_{10}^{6+} chromophores have identical spectra with absorption/emission maxima at 490/570 nm (Figure 1).[35] Within these binding sites, the X nucleobase is a linchpin ligand because this chromophore does not form with other canonical nucleobases. More specifically, its functional groups control the electronic environment because the adducts with X = I vs G is 2.5× brighter (Q_F = 63% vs 25%) and the amplitude-weighted emission lifetime is almost 2× longer (see below).[35]

We probe these two guest−host complexes using TRIR spectroscopy (see the SI for full experimental details). All TRIR measurements were performed on buffered D_2O solutions because of this solvent's superior IR transmission. The transient spectra reveal rich patterns of positive and negative peaks when the cluster is electronically excited in the visible (Figure 2). Because a bare cluster of heavy Ag atoms has vibrations that are <200 cm^{-1} in frequency,[40] all bands in Figure 2 are due to nucleobase vibrations, possibly perturbed by metal−ligand interactions. As discussed below, the negative bands correspond to bleaching of nucleobase vibrations, but this bleaching cannot result from nucleobase-localized excited states, which lie too high in energy to be reached by the 490 nm pump pulse.

The TRIR signals were globally fit to biexponential functions at delay times between 0.5 ps and 3.5 ns. At nearly all probe frequencies, the TRIR signals are dominated by longer-lived components of 2.0 ± 0.1 and 3.2 ± 0.1 ns for G-AgC and I-AgC, respectively (Figure 2c,d and Figure S2), as shown by the kinetics of the most intense negative band at 1623 cm^{-1} (band 3′; Figures 3 and S3). These decay times mirror the respective amplitude-weighted visible emission lifetimes of 1.9 ± 0.3 and 3.4 ± 0.1 ns.[35] Thus, the synchronous decay of the mid-infrared absorption and visible emission signals indicates that the vibrational modes of the encapsulating nucleobases are populated solely because the cluster is photoexcited. It is unlikely that the bleaching of the DNA vibrational modes is due to electronic-to-vibrational energy transfer (EVET), a resonant dipolar energy transfer mechanism.[41] This is because the ns lifetimes observed here are much longer than vibrational excited states of nucleobases, which are expected to decay in several ps in aqueous solution.[42]

The rise of the TRIR bands is instrument-limited, and signals like the ones in Figure 3 change from 10% to 90% of

https://dx.doi.org/10.1021/acs.jpclett.0c02486
J. Phys. Chem. Lett. 2020, 11, 8958−8963

Table 1. Major Band Positions in the FTIR Spectra and Negative-Going GSB Bands in the TRIR Spectra of I-AgC and G-AgC[a]

		bands (cm^{-1})						
I-AgC	FTIR	1692 (1)	1657 (2)		1635 (3)		1535 (4)	1506 (5)
	TRIR		1660 (2′)	1648 (a′)	1623 (3′)		1545 (4′)	1512 (5′)
G-AgC	FTIR	1692 (1)	1657 (2)		1638 (3)		1535 (4)	1506 (5)
	TRIR		1662 (2′)	1642 (a′)	1623 (3′)	1580 (b′)	1542 (4′)	1512 (5′)

[a]Number and letters in parentheses refer to labels for the bands in Figure 2. Estimated uncertainties in reported frequencies are ±2 cm^{-1} (2σ).

their peak values in 400 fs, which is thus an upper limit on the formation time of the emissive excited state or states. Intriguingly, most of the negative bands increase by an additional 10−20% with a time constant of ∼6 ps as shown in Figure 3 for band 3′. The delayed growth of the bleach signals requires further study, but it is unlikely to reflect growth of the emissive state population on the same time scale, because the positive bands that decay in unison with the emission do not show this component (e.g., the 1596 cm^{-1} band in Figure 3). The positive bands are potentially rich in information, but their analysis is more difficult as the precise species responsible cannot be identified without calculations, which go beyond the scope of this study.

To decipher the bonding within the Ag_{10}^{6+} coordination site, we focus on the negative-going, ground-state bleaching vibrational modes because they can be assigned based on corresponding transitions in the steady-state FTIR spectra. The FTIR spectra of I- and G-AgC are similar and display five major bands (Table 1 and inverted black curves in Figure 2a,b). Cytidine and thymidine transitions dominate these spectra because they comprise 16 of the 18 nucleosides.

Band 1 is attributed to thymidine, which has the highest frequency C═O stretching band of all the nucleosides (Figure S4). Bands 2−5 fall in the spectral region for cytidine, as 5′-CMP in D_2O has resonances at 1650, 1617, 1522, and 1504 cm^{-1} (Figure S4), and its Ag^+ complex exhibits corresponding transitions at 1652, 1618, 1530, and 1507 cm^{-1}.[43] Of these four peaks, the 1522 → 1530 cm^{-1} shift is the largest, presumably because Ag^+ coordinates with the cytidine N3 and alters the C═N stretching frequency.[43] We observe analogous transitions at 1657 (band 2), 1638 (band 3), 1535 (band 4), and 1506 (band 5) cm^{-1} for G-AgC and similar frequencies for I-AgC (Table 1 and Figure S5). Band 2 at 1657 cm^{-1} in each DNA-AgC agrees well with the 1652 cm^{-1} band of Ag(I)-cytidine and the 1650 cm^{-1} band of 5′-CMP. Band 3 at ∼1638 cm^{-1} is upshifted compared to the 1618 cm^{-1} band of Ag(I)-cytidine, possibly because it overlaps with the 1632 cm^{-1} transition for thymidine (Figure S4).[44] Bands 4 and 5 fall in the 1500 to 1550 cm^{-1} window where only cytidine has resonances in D_2O (Figure S4).[45]

These FTIR band assignments were then used to understand the TRIR spectra, and we focus on the quartet of negative peaks labeled 2′−5′ (Figure 2 c,d). Bands 2′, 4′, and 5′ are upshifted by 3−10 cm^{-1} compared to the FTIR bands 2, 4, and 5 (Table 1), possibly due to overlapping positive bands on the low frequency side of each peak. In contrast, band 3′ at 1623 cm^{-1} is downshifted more than 10 cm^{-1} from the corresponding band 3 in the FTIR spectra and more closely matches the 1618 cm^{-1} band reported for the Ag(I)-cytidine complex.[43] We suggest that the TRIR spectra resolve the overlapping cytidine and thymidine transitions in band 3 because cytidine preferentially coordinates the cluster.[46,47]

To further support the selectivity of the TRIR spectra, we consider band 1 in the FTIR spectrum. This thymidine C═O transition is absent in the TRIR spectra, which is surprising given that thymidine comprises 5 of the 18 nucleosides in the two sequences. This difference indicates that the thymidines in G- and I-AgC are not perturbed when the cluster is electronically excited, possibly because they weakly coordinate the cluster. Prior studies demonstrate that thymidine is a poor ligand for silver clusters because its N3 coordination site is blocked at neutral pH.[48] This site can be deprotonated at high pH (≳ 10) to form fluorescent clusters, and such pH-dependent spectral changes are reversible.[49] Additionally, spectroscopic studies of a broad range of oligonucleotides with different sequences indicate that thymidine favors clusters with weak emission.[50] Furthermore, thymidine can be enzymatically excised and thus completely removed from the DNA backbone without disturbing the cluster environment.[35] Thus, we suggest that the thymidines do not yield transient spectra because they do not coordinate the cluster. This suggests further that the TRIR spectra are due to bonding interactions and not due to the vibrational Stark effect, which would perturb the global electrostatic environment and hence shift the vibrations of the IR-active oscillators of the nucleobases in a less specific manner.[51]

TRIR selectivity for bonded nucleobases is suggested by the band positions and intensity of bands a′ and b′ in the transient spectra. While the frequencies of bands 2′−5′ differ by ≲3 cm^{-1} for the X = G and I complexes, band a′ at 1642 cm^{-1} for G-AgC is distinct from its counterpart at 1648 cm^{-1} for I-AgC (Table 1). The magnitude and direction of this 6 cm^{-1} shift is consistent with vibrational changes between guanosine and inosine. The a′ band is possibly due to bleaching of the carbonyl group of base X, which has a frequency of 1663 cm^{-1} for 5′-GMP and 1673 cm^{-1} for hypoxanthine, the nucleobase of inosine (Figure S6; hypoxanthine, inosine, and 5′-IMP have almost indistinguishable FTIR spectra in the 1400−1720 cm^{-1} region).[52,53] The 20 to 25 cm^{-1} downshift of the carbonyl bleach frequencies of X in the DNA-AgC may indicate a slight loss of C═O character when X binds to Ag(I) or Ag(0) via one of the N atoms or the carbonyl group. A downshift in frequency due to the loss of double bond character upon metal ion binding is seen when 1-methylthymine binds to *cis*-$Pt(NH_3)_2^{2+}$ and Ag^+ ions.[54]

To substantiate the identification of guanosine, the negative-going band b′ at 1580 cm^{-1} is observed with G-AgC but not with I-AgC (Figure 2 and Table 1). This observation is again consistent with the behavior of the nucleobases. Band b′ in G-AgC matches the frequency of the ring in-plane stretch vibration of guanosine, but this same transition in inosine is substantially weaker (Figure S6). Additionally, this transition is a signature of guanosine because the other canonical bases do not have strong IR bands around 1580 cm^{-1} (Figure S4).[45]

The guanosine may coordinate via its different electron-rich heteroatoms, such as the deprotonated N1, the N7, and/or the C6═O.[46,55−59] N1 coordination in our complexes is eliminated based on the TRIR spectroscopy. First, strong

https://dx.doi.org/10.1021/acs.jpclett.0c02486
J. Phys. Chem. Lett. 2020, 11, 8958−8963

evidence suggests that the a′ bands in Figure 2 are due to carbonyl stretching of G with a hydrogen atom bound to N1, possibly perturbed by cluster binding, as discussed above. Second, the FTIR spectrum of the N1-deprotonated GMP (G(−H1$^+$)) (Figure S4b, dashed curve) has a strong band between 1450 and 1500 cm^{-1} that is not seen for the neutral base. The absence of any significant signals in this region makes bleaching of bands due to G(−H1$^+$) very unlikely.

It is remarkable that bleaching of X = G/I is observed even though it is only 1 of the 18 nucleosides, and the corresponding vibrational bands are undetectable in the FTIR spectra. As with the bleach bands observed for cytidine, but not for thymidine, this bleach signal suggests that guanosine and inosine coordinate the cluster and are perturbed when the cluster is electronically excited. Despite the 11:1 mol ratio of cytidine to X, the amplitude of the bleached X band is more than half as large as that of the nearby bands 2′ and 3′, which are assigned to cytidine. This may indicate that only a subset of all cytidines interacts with the excited cluster, but more study is needed to determine how many and which cytidines are cluster-bound.

The rich pattern of positive and negative bands seen in the TRIR spectra in Figure 2 is similar to that observed when exciting bare DNA strands with UV radiation.[60−62] In these studies, the positive bands occur at frequencies close to ones calculated for various nucleobase radical ions, providing evidence that photoexcitation forms charge transfer (CT) states. If CT states were to form in DNA-AgCs, then the vibrational frequencies of the nucleobase ions could shift due to metal cluster coordination, complicating their identification. CT states of DNA-AgCs have been discussed previously,[18] but Lippert-Mataga models may not accurately describe the emission solvatochromism observed in water−alcohol mixed solvents.[63] Further study is needed to ascertain the degree to which any level of CT is present along with whether the shifts in nucleobase fundamentals can be explained alternatively by changes in ligand binding arising from non-CT excited states of the cluster-DNA complex.

In summary, TRIR spectra of two visible emissive DNA-AgCs show that electronic excitation of the encapsulated cluster bleaches the vibrational modes of a subset of the nucleobases. These vibrational signatures decay synchronously as the cluster electronically relaxes and show that the cluster is strongly coupled with specific nucleobases within the polydentate DNA ligand. It may be possible to characterize the coordination sites of a wide range of these complexes via TRIR spectroscopy with UV, visible, or NIR excitation. For example, our experiments identify spectral signatures of a subset of all cytidines but not thymidine. Furthermore, it is remarkable that the single guanosine/inosine, with information on the (de)protonation state, can be identified in the TRIR spectra. Such vibrational signatures could be used to understand the bonding which ultimately controls the electronic spectra of DNA-silver cluster chromophores.

■ ASSOCIATED CONTENT

Supporting Information

The Supporting Information is available free of charge at https://pubs.acs.org/doi/10.1021/acs.jpclett.0c02486.

Synthesis and methods description, additional TRIR results, and FTIR spectra of DNA nucleobase monomers (PDF)

■ AUTHOR INFORMATION

Corresponding Authors

Jeffrey T. Petty − *Department of Chemistry, Furman University, Greenville, South Carolina 29613, United States;* orcid.org/0000-0003-0149-5335; Phone: +1 864-294-2689; Email: jeff.petty@furman.edu

Bern Kohler − *Department of Chemistry and Biochemistry, The Ohio State University, Columbus, Ohio 43210, United States;* orcid.org/0000-0001-5353-1655; Phone: +1 614-688-2635; Email: kohler.40@osu.edu

Authors

Yuyuan Zhang − *Department of Chemistry and Biochemistry, The Ohio State University, Columbus, Ohio 43210, United States*

Chen He − *Department of Chemistry, Furman University, Greenville, South Carolina 29613, United States;* orcid.org/0000-0001-5426-769X

Complete contact information is available at: https://pubs.acs.org/10.1021/acs.jpclett.0c02486

Notes

Any opinions, findings, and conclusions or recommendations expressed in this material are those of the author(s) and do not necessarily reflect those of the National Science Foundation. The authors declare no competing financial interest.

■ ACKNOWLEDGMENTS

Work at The Ohio State University was supported by the U.S. National Science Foundation (CHE-1800471) and by funding from The Ohio State University. Work at Furman was supported by the National Science Foundation (CHE-1611451 and CHE-2002910) and the Furman Advantage program. This work was supported in part by the National Science Foundation EPSCoR Program under NSF Award No. OIA-1655740.

■ REFERENCES

(1) Kubo, R. Electronic Properties of Metallic Fine Particles. I. *J. Phys. Soc. Jpn.* **1962**, *17*, 975−986.

(2) Kubo, R.; Kawabata, A.; Kobayashi, S. Electronic-Properties of Small Particles. *Annu. Rev. Mater. Sci.* **1984**, *14*, 49−66.

(3) Zheng, J.; Nicovich, P. R.; Dickson, R. M. Highly Fluorescent Noble-Metal Quantum Dots. *Annu. Rev. Phys. Chem.* **2007**, *58*, 409−431.

(4) Gell, L.; Kulesza, A.; Petersen, J.; Rohr, M. I. S.; Mitrić, R.; Bonačić-Koutecký, V. Tuning Structural and Optical Properties of Thiolate-Protected Silver Clusters by Formation of a Silver Core with Confined Electrons. *J. Phys. Chem. C* **2013**, *117*, 14824−14831.

(5) Aikens, C. M. Electronic and Geometric Structure, Optical Properties, and Excited State Behavior in Atomically Precise Thiolate-Stabilized Noble Metal Nanoclusters. *Acc. Chem. Res.* **2018**, *51*, 3065−3073.

(6) Henglein, A.; Mulvaney, P.; Linnert, T. Chemistry of Ag_n Aggregates in Aqueous-Solution - Nonmetallic Oligomeric Clusters and Metallic Particles. *Faraday Discuss.* **1991**, *92*, 31−44.

(7) Rabin, I.; Schulze, W.; Ertl, G. Absorption Spectra of Small Silver Clusters Ag_n ($n \geq 3$). *Chem. Phys. Lett.* **1999**, *312*, 394−398.

(8) Zheng, J.; Dickson, R. M. Individual Water-Soluble Dendrimer-Encapsulated Silver Nanodot Fluorescence. *J. Am. Chem. Soc.* **2002**, *124*, 13982−13983.

(9) Petty, J. T.; Zheng, J.; Hud, N. V.; Dickson, R. M. DNA-templated Ag Nanocluster Formation. *J. Am. Chem. Soc.* **2004**, *126*, 5207−5212.

(10) Richards, C. I.; Choi, S.; Hsiang, J. C.; Antoku, Y.; Vosch, T.; Bongiorno, A.; Tzeng, Y. L.; Dickson, R. M. Oligonucleotide-Stabilized Ag Nanocluster Fluorophores. *J. Am. Chem. Soc.* **2008**, *130*, 5038−5039.
(11) Yeh, H. C.; Sharma, J.; Han, J. J.; Martinez, J. S.; Werner, J. H. A DNA-Silver Nanocluster Probe That Fluoresces upon Hybridization. *Nano Lett.* **2010**, *10*, 3106−3110.
(12) Petty, J. T.; Sengupta, B.; Story, S. P.; Degtyareva, N. N. DNA Sensing by Amplifying the Number of Near-Infrared Emitting, Oligonucleotide-Encapsulated Silver Clusters. *Anal. Chem.* **2011**, *83*, 5957−5964.
(13) Yang, S. W.; Vosch, T. Rapid Detection of MicroRNA by a Silver Nanocluster DNA Probe. *Anal. Chem.* **2011**, *83*, 6935−6939.
(14) Copp, S. M.; Schultz, D.; Swasey, S.; Pavlovich, J.; Debord, M.; Chiu, A.; Olsson, K.; Gwinn, E. Magic Numbers in DNA-Stabilized Fluorescent Silver Clusters Lead to Magic Colors. *J. Phys. Chem. Lett.* **2014**, *5*, 959−963.
(15) Obliosca, J. M.; Liu, C.; Yeh, H. C. Fluorescent Silver Nanoclusters as DNA Probes. *Nanoscale* **2013**, *5*, 8443−8461.
(16) Yu, J. H.; Choi, S. M.; Richards, C. I.; Antoku, Y.; Dickson, R. M. Live Cell Surface Labeling with Fluorescent Ag Nanocluster Conjugates. *Photochem. Photobiol.* **2008**, *84*, 1435−1439.
(17) Copp, S. M.; Schultz, D. E.; Swasey, S.; Gwinn, E. G. Atomically Precise Arrays of Fluorescent Silver Clusters: A Modular Approach for Metal Cluster Photonics on DNA Nanostructures. *ACS Nano* **2015**, *9*, 2303−2310.
(18) Patel, S. A.; Cozzuol, M.; Hales, J. M.; Richards, C. I.; Sartin, M.; Hsiang, J. C.; Vosch, T.; Perry, J. W.; Dickson, R. M. Electron Transfer-Induced Blinking in Ag Nanodot Fluorescence. *J. Phys. Chem. C* **2009**, *113*, 20264−20270.
(19) Cerretani, C.; Carro-Temboury, M. R.; Krause, S.; Bogh, S. A.; Vosch, T. Temperature Dependent Excited State Relaxation of a Red Emitting DNA-templated Silver Nanocluster. *Chem. Commun.* **2017**, *53*, 12556−12559.
(20) Sharma, J.; Yeh, H. C.; Yoo, H.; Werner, J. H.; Martinez, J. S. A Complementary Palette of Fluorescent Silver Nanoclusters. *Chem. Commun.* **2010**, *46*, 3280−3282.
(21) Schultz, D.; Gardner, K.; Oemrawsingh, S. S. R.; Markesevic, N.; Olsson, K.; Debord, M.; Bouwmeester, D.; Gwinn, E. Evidence for Rod-Shaped DNA-Stabilized Silver Nanocluster Emitters. *Adv. Mater.* **2013**, *25*, 2797−2803.
(22) Richards, C. I.; Hsiang, J. C.; Senapati, D.; Patel, S.; Yu, J. H.; Vosch, T.; Dickson, R. M. Optically Modulated Fluorophores for Selective Fluorescence Signal Recovery. *J. Am. Chem. Soc.* **2009**, *131*, 4619−4621.
(23) Petty, J. T.; Fan, C. Y.; Story, S. P.; Sengupta, B.; Iyer, A. S.; Prudowsky, Z.; Dickson, R. M. DNA Encapsulation of 10 Silver Atoms Producing a Bright, Modulatable, Near-Infrared-Emitting Cluster. *J. Phys. Chem. Lett.* **2010**, *1*, 2524−2529.
(24) Petty, J. T.; Fan, C. Y.; Story, S. P.; Sengupta, B.; Sartin, M.; Hsiang, J. C.; Perry, J. W.; Dickson, R. M. Optically Enhanced, Near-IR, Silver Cluster Emission Altered by Single Base Changes in the DNA Template. *J. Phys. Chem. B* **2011**, *115*, 7996−8003.
(25) Fleischer, B. C.; Petty, J. T.; Hsiang, J. C.; Dickson, R. M. Optically Activated Delayed Fluorescence. *J. Phys. Chem. Lett.* **2017**, *8*, 3536−3543.
(26) Krause, S.; Carro-Temboury, M. R.; Cerretani, C.; Vosch, T. Anti-Stokes Fluorescence Microscopy Using Direct and Indirect Dark State Formation. *Chem. Commun.* **2018**, *54*, 4569−4572.
(27) Yau, S. H.; Abeyasinghe, N.; Orr, M.; Upton, L.; Varnavski, O.; Werner, J. H.; Yeh, H. C.; Sharma, J.; Shreve, A. P.; Martinez, J. S.; et al. Bright Two-Photon Emission and Ultra-Fast Relaxation Dynamics in a DNA-Templated Nanocluster Investigated by Ultra-Fast Spectroscopy. *Nanoscale* **2012**, *4*, 4247−4254.
(28) Thyrhaug, E.; Bogh, S. A.; Carro-Temboury, M. R.; Madsen, C. S.; Vosch, T.; Zigmantas, D. Ultrafast Coherence Transfer in DNA-Templated Silver Nanoclusters. *Nat. Commun.* **2017**, *8*, 15577.
(29) Reveguk, Z.; Lysenko, R.; Ramazanov, R.; Kononov, A. Ultrafast Fluorescence Dynamics of DNA-based Silver Clusters. *Phys. Chem. Chem. Phys.* **2018**, *20*, 28205−28210.
(30) Volkov, I. L.; Reveguk, Z. V.; Serdobintsev, P. Y.; Ramazanov, R. R.; Kononov, A. I. DNA as UV Light-Harvesting Antenna. *Nucleic Acids Res.* **2018**, *46*, 3543−3551.
(31) O'Neill, P. R.; Gwinn, E. G.; Fygenson, D. K. UV Excitation of DNA Stabilized Ag Cluster Fluorescence via the DNA Bases. *J. Phys. Chem. C* **2011**, *115*, 24061−24066.
(32) Soto-Verdugo, V.; Metiu, H.; Gwinn, E. The Properties of Small Ag Clusters Bound to DNA Bases. *J. Chem. Phys.* **2010**, *132*, 195102.
(33) Longuinhos, R.; Lucio, A. D.; Chacham, H.; Alexandre, S. S. Charge-transfer Optical Absorption Mechanism of DNA:Ag-nanocluster Complexes. *Phys. Rev. E: Stat. Phys., Plasmas, Fluids, Relat. Interdiscip. Top.* **2016**, *93*, No. 052413.
(34) Chen, X.; Boero, M.; Lopez-Acevedo, O. Atomic Structure and Origin of Chirality of DNA-Stabilized Silver Clusters. *Phys. Rev. Mater.* **2020**, *4*, No. 065601.
(35) Petty, J. T.; Ganguly, M.; Yunus, A. I.; He, C.; Goodwin, P. M.; Lu, Y. H.; Dickson, R. M. A DNA-Encapsulated Silver Cluster and the Roles of Its Nucleobase Ligands. *J. Phys. Chem. C* **2018**, *122*, 28382−28392.
(36) Petty, J. T.; Sergev, O. O.; Kantor, A. G.; Rankine, I. J.; Ganguly, M.; David, F. D.; Wheeler, S. K.; Wheeler, J. F. Ten-Atom Silver Cluster Signaling and Tempering DNA Hybridization. *Anal. Chem.* **2015**, *87*, 5302−5309.
(37) Petty, J. T.; Sergev, O. O.; Ganguly, M.; Rankine, I. J.; Chevrier, D. M.; Zhang, P. A Segregated, Partially Oxidized, and Compact Ag_{10} Cluster within an Encapsulating DNA Host. *J. Am. Chem. Soc.* **2016**, *138*, 3469−3477.
(38) Petty, J. T.; Ganguly, M.; Rankine, I. J.; Chevrier, D. M.; Zhang, P. A DNA-Encapsulated and Fluorescent Ag_{10}^{6+} Cluster with a Distinct Metal-Like Core. *J. Phys. Chem. C* **2017**, *121*, 14936−14945.
(39) He, C.; Goodwin, P. M.; Yunus, A. I.; Dickson, R. M.; Petty, J. T. A Split DNA Scaffold for a Green Fluorescent Silver Cluster. *J. Phys. Chem. C* **2019**, *123*, 17588−17597.
(40) Mancera, L. A.; Benoit, D. M. Vibrational Anharmonicity of Small Gold and Silver Clusters Using the VSCF Method. *Phys. Chem. Chem. Phys.* **2016**, *18*, 529−549.
(41) Peterson, M. D.; Cass, L. C.; Harris, R. D.; Edme, K.; Sung, K.; Weiss, E. A. The Role of Ligands in Determining the Exciton Relaxation Dynamics in Semiconductor Quantum Dots. *Annu. Rev. Phys. Chem.* **2014**, *65*, 317−339.
(42) Zhang, Y.; Chen, J.; Kohler, B. Hydrogen Bond Donors Accelerate Vibrational Cooling of Hot Purine Derivatives in Heavy Water. *J. Phys. Chem. A* **2013**, *117*, 6771−6780.
(43) Goncharova, I. Ag(I)-Mediated Homo and Hetero Pairs of Guanosine and Cytidine: Monitoring by Circular Dichroism Spectroscopy. *Spectrochim. Acta, Part A* **2014**, *118*, 221−227.
(44) Banyay, M.; Sarkar, M.; Gräslund, A. A Library of IR Bands of Nucleic Acids in Solution. *Biophys. Chem.* **2003**, *104*, 477−488.
(45) Peng, C. S.; Jones, K. C.; Tokmakoff, A. Anharmonic Vibrational Modes of Nucleic Acid Bases Revealed by 2D IR Spectroscopy. *J. Am. Chem. Soc.* **2011**, *133*, 15650−15660.
(46) Cerretani, C.; Kanazawa, H.; Vosch, T.; Kondo, J. Crystal Structure of a NIR-Emitting DNA-Stabilized Ag_{16} Nanocluster. *Angew. Chem., Int. Ed.* **2019**, *58*, 17153−17157.
(47) Huard, D. J. E.; Demissie, A.; Kim, D.; Lewis, D.; Dickson, R. M.; Petty, J. T.; Lieberman, R. L. Atomic Structure of a Fluorescent Ag_8 Cluster Templated by a Multistranded DNA Scaffold. *J. Am. Chem. Soc.* **2019**, *141*, 11465−11470.
(48) Sengupta, B.; Ritchie, C. M.; Buckman, J. G.; Johnsen, K. R.; Goodwin, P. M.; Petty, J. T. Base-Directed Formation of Fluorescent Silver Clusters. *J. Phys. Chem. C* **2008**, *112*, 18776−18782.
(49) Ganguly, M.; Bradsher, C.; Goodwin, P.; Petty, J. T. DNA-Directed Fluorescence Switching of Silver Clusters. *J. Phys. Chem. C* **2015**, *119*, 27829−27837.

https://dx.doi.org/10.1021/acs.jpclett.0c02486
J. Phys. Chem. Lett. 2020, 11, 8958−8963

(50) Copp, S. M.; Bogdanov, P.; Debord, M.; Singh, A.; Gwinn, E. Base Motif Recognition and Design of DNA Templates for Fluorescent Silver Clusters by Machine Learning. *Adv. Mater.* **2014**, *26*, 5839−5845.
(51) Fried, S. D.; Boxer, S. G. Measuring Electric Fields and Noncovalent Interactions Using the Vibrational Stark Effect. *Acc. Chem. Res.* **2015**, *48*, 998−1006.
(52) Psoda, A.; Shugar, D. Spectral Studies on Tautomeric Forms of Inosine. *Biochim. Biophys. Acta, Nucleic Acids Protein Synth.* **1971**, *247*, 507−513.
(53) Tajmir-Riahi, H. A.; Theophanides, T. An FT-IR Study of *cis*-Dichlorodiammineplatinum(II) and *trans*-Dichlorodiammineplatinum(II) Bound to Inosine-5′-Monophosphate. *Can. J. Chem.* **1984**, *62*, 1429−1440.
(54) Lippert, B.; Neugebauer, D. Simultaneous Binding of Two Different Transition-Metals to the DNA Model Base 1-Methylthymine: The X-Ray Structure of Bis[Bis(μ-1-Methylthyminato-N3,O4)-Cis-Diammine Platinum(II)] Silver-Nitrate Pentahydrate. *Inorg. Chim. Acta* **1980**, *46*, 171−179.
(55) Tu, A. T.; Reinosa, J. A. Interaction of Silver Ion with Guanosine Guanosine Monophosphate and Related Compounds. Determination of Possible Sites of Complexing. *Biochemistry* **1966**, *5*, 3375−3383.
(56) Matsuoka, Y.; Nordén, B.; Kurucsev, T. Nucleic-Acid Metal Interactions. 2. Complexes of Silver(I) with Guanosine and 7-Methylguanine from Studies of Isotropic and Dichroic Spectra. *J. Phys. Chem.* **1984**, *88*, 971−976.
(57) Menzer, S.; Hillgeris, E. C.; Lippert, B. Preparation, X-Ray Structure and Solution Behavior of $[Ag(9\text{-EtGH-}N7)_2]NO_3\cdot H_2O$ (9-EtGH = 9-Ethylguanine). *Inorg. Chim. Acta* **1993**, *210*, 167−171.
(58) Loo, K.; Degtyareva, N.; Park, J.; Sengupta, B.; Reddish, M.; Rogers, C. C.; Bryant, A.; Petty, J. T. Ag^+-Mediated Assembly of 5′-Guanosine Monophosphate. *J. Phys. Chem. B* **2010**, *114*, 4320−4326.
(59) Swasey, S. M.; Leal, L. E.; Lopez-Acevedo, O.; Pavlovich, J.; Gwinn, E. G. Silver (I) as DNA Glue: Ag^+-mediated Guanine Pairing Revealed by Removing Watson-Crick Constraints. *Sci. Rep.* **2015**, *5*, 10163.
(60) Doorley, G. W.; Wojdyla, M.; Watson, G. W.; Towrie, M.; Parker, A. W.; Kelly, J. M.; Quinn, S. J. Tracking DNA Excited States by Picosecond-Time-Resolved Infrared Spectroscopy: Signature Band for a Charge-Transfer Excited State in Stacked Adenine-Thymine Systems. *J. Phys. Chem. Lett.* **2013**, *4*, 2739−2744.
(61) Bucher, D. B.; Pilles, B. M.; Carell, T.; Zinth, W. Charge Separation and Charge Delocalization Identified in Long-Living States of Photoexcited DNA. *Proc. Natl. Acad. Sci. U. S. A.* **2014**, *111*, 4369−4374.
(62) Zhang, Y.; Dood, J.; Beckstead, A. A.; Li, X.-B.; Nguyen, K. V.; Burrows, C. J.; Improta, R.; Kohler, B. Efficient UV-Induced Charge Separation and Recombination in an 8-Oxoguanine-Containing Dinucleotide. *Proc. Natl. Acad. Sci. U. S. A.* **2014**, *111*, 11612−11617.
(63) Copp, S. M.; Faris, A.; Swasey, S. M.; Gwinn, E. G. Heterogeneous Solvatochromism of Fluorescent DNA-Stabilized Silver Clusters Precludes Use of Simple Onsager-Based Stokes Shift Models. *J. Phys. Chem. Lett.* **2016**, *7*, 698−703.

https://dx.doi.org/10.1021/acs.jpclett.0c02486
J. Phys. Chem. Lett. 2020, 11, 8958−8963